Glycoconjugate Journal (1997) **14:** 951–961

EGC1
Synergistic gelation of xanthan gum with locust bean gum: a rheological investigation

Giuliano Copetti, Mario Grassi, Romano Lapasin and Sabrina Pricl*

Department of Chemical, Environmental and Raw Materials Engineering – DICAMP, University of Trieste, Piazzale Europa 1, I-34127 Trieste, Italy

Many industrial products often include in their formulation more than one polysaccharide to achieve the desired properties during and after processing. Many such mixed systems behave as would be expected from the known properties of the individual polymers. In others, however, their properties are superior to those of either component alone, or may be qualitatively different. In many polysaccharide systems, the combination of a gelling polymer with a nongelling one gives rise to strong synergistic effects, as a consequence of interaction among different chain polymers and formation of mixed junction zones.

Probably, the most exploited mixed gels, especially by the food industry, are those involving the microbial polysaccharide xanthan gum (XG) and the plant galactomannans, like locust bean gum (LBG). Concentrated aqueous systems of LBG and XG display quite different rheological properties: the former show the behaviour typical of hyperentangled macromolecular solutions, whereas the flow and viscoelastic properties of XG systems correspond to those of tenuous, weak-gel networks. Interestingly, when mixed together these macromolecules interact to form a firm, thermoreversible gel with synergistic effects.

In the present paper we report the results of a thorough investigation of both polymer concentration and temperature effects on the rheological properties of mixed LBG-XG systems in 20 mM KCl under continuous and oscillatory flow conditions.

Under continuous shear at 25 °C, pure LBG shows the flow properties of a macromolecular solution, with a shear-thinning behaviour and a Newtonian region at low shear rates, whereas the rheological behaviour of XG and all LX mixed systems is that typical of weak-gels. Furthermore, in the mixed systems the viscosity values do not increase monotonically with increasing xanthan concentration, but the synergistic effect has a maximum in accordance with the XG : LBG ratio 1 : 1. As the temperature is increased from 25 °C to 85 °C, whilst the LBG system do not show any qualitative change but there is only a parallel, downward shift of viscosity values, in the case of xanthan there is a dramatic change in the corresponding curve profiles, due to the thermally induced helix-coil conformational transition.

The differences in the rheological behaviour of the systems examined can be better shown through dynamic tests at 25 °C. The strain sweeps performed at constant frequency of oscillation reveal that the mixed systems show higher sensitivity to strain amplitude, and lower strain values must be attained to ensure linear viscoelastic properties. The mechanical spectra clearly show the influence of composition on the viscoelastic properties of these biopolymer systems. All LX systems show the mechanical spectra typical of polysaccharide gels: G' is always much greater than G'' and is nearly independent of the applied frequency over a wide frequency range. In addition, the marked gap between the elastic responses of the pure LBG and the LX 1 : 3 systems demonstrates the strong effect of the initial addition of xanthan to the pure LBG, especially in the low frequency range, whereas the highest synergistic effect is attained for the LX 1 : 1 system. A comprehensive description of the frequency dependence of both moduli can be suitably obtained through the four-parameter Friedrich model, which belongs to the class of fractional derivative approaches viscoelasticity.

The same thermal effect is observed for the XG and all LX mixed systems considered, indicating a progressive change from the behaviour of a typical gel to that of a quasi-solution state, when temperature is increased from 25 °C to 85 °C. Among all mixed systems, the LX 1 : 1 has the highest values of the moduli at any temperature considered, and is characterized by the highest gel-sol transition temperature. In all LX systems, the temperature sweeps show that the gel-sol transition follows a two-step process, characterized by the presence of two inflection points in the relevant G^* *vs* T curves. The first step could be reasonably ascribed to the melting process of the mixed xanthan-locust bean gum junction zones, in which the association of XG with LBG is occurring with the xanthan component in its fully ordered helical conformation. The second step, occurring at higher temperature, can be attributed to the conformational transition of the xanthan chains.

*To whom correspondence should be addressed.

0282–0080

All the experimental results from this study seem to suggest the coexistence, within the structure of these mixed gels, of both heterotypic LBG-XG and homotypic XG-XG junction zones, in which the xanthan chains retain their ordered helical conformation, thus supporting the original model proposed by Dea and Morris.

***Keywords*: xanthan gum, locust bean gum, mixed gels, synergism, rheology, thermal effects, viscoelasticity, gelation mechanism, helix-coil transition, Friedrich model**

Introduction

The impact of polysaccharides in industrial applications is enormous. The usefulness of these water-soluble carbohydrate polymers in industry undoubtedly relies on the wide range of their functional properties. Chief among polysaccharide characteristics is their ability to modify the properties of aqueous environments, that is their capacity to thicken, chelate, emulsify, stabilize, encapsulate, flocculate, swell and suspend, or to form gels, films and membranes.

Polysaccharides are biopolymers from renewable sources; therefore, peculiar features like biocompatibility, biodegradability, bioadhesivity and nontoxicity, coupled with wide availability and usually low costs, account for their steadily increasing exploitation in the formulation of products for food, biomedical and cosmetic applications.

In many natural systems, different polysaccharides are often present at the same time in the same environment, where they all contribute – in the solid, solution or gel state – to the specific biological purpose of achieving the necessary physical structure. Industrially, there is a growing interest in the formulation of mixed polysaccharide systems, leading to final products having specific properties and possibly cost advantages; many such mixed systems already find extensive food applications.

Generally, blends of two or more polysaccharides exhibit complex and often spectacular properties, which depend not only on total polymer concentration, relative proportions of polymeric components, solvent medium characteristics and temperature, but also on the thermal and mechanical history experienced by the systems themselves. The reasons for such complexities can be traced to the efficiency of the interactions which can take place between the biopolymer molecules, and to the balance existing between self- and mutual interactions, which is a function of the different primary and secondary structures of the component chains.

The result is that a wide variety of structural conditions is encountered in mixed polysaccharide systems, and that a strong nonlinearity of the macroscopic properties is inevitably observed. Indeed, there are many cases in which polymer mixing gives gels characterized by high rigidity, superior to that which would be expected from a linear combination of the rigidities of the gels formed by each individual polymeric component. In other situations, the addition of a small amount of a nongelling polymer to a gelling one may induce a strengthening of the resulting gel or, even, some polymers that are individually nongelling can yield gels on mixing. Many such polysaccharide mixed systems show this nonadditive behaviour, which is currently termed synergism.

Synergistic gel formation can occur in a number of ways. Intermolecular interactions can have a chemical origin, with covalent bond formation between the participating polymer chains, as we observe for propylene glycol alginate and gelatin under mild alkaline conditions. In such cases, the result is the formation of a chemical gel network [1]. More frequently, when polysaccharides are concerned, physical intermolecular interactions occur, either involving cooperative associations of chain segments belonging to different polymers in the formation of mixed junction zones, analogues to the junctions in many single-component gel systems [2], or via chain-chain association by virtue of opposite charge attractions [3]. In many cases, however, the behaviour of a mixed polymer system is governed by thermodynamically unfavourable ($\Delta H < 0$) segment–segment interactions, which eventually lead to mutual exclusion effects of each component from the polymer domain of the other, thus increasing the effective concentration of both. When thermodynamic incompatibility is the main principle governing the structural state of a system, beyond a certain concentration value of one component the system separates into two phases, giving a route to the formation of the so-called phase-separated or multitextured gels. Lastly, it is also possible for mixed systems to give the deceptive appearance of polymer synergism when the effective interaction is between one of the polymers and small molecules or ions present on the other polymer sample or in the environment.

It has been known for some years that the weak gel properties of xanthan gum (XG), the well-known exocellular microbial polysaccharide (see Figure 1), are enhanced by the presence of certain β-1,4 linked plant polysaccharides of a type which normally exist in water solution as random

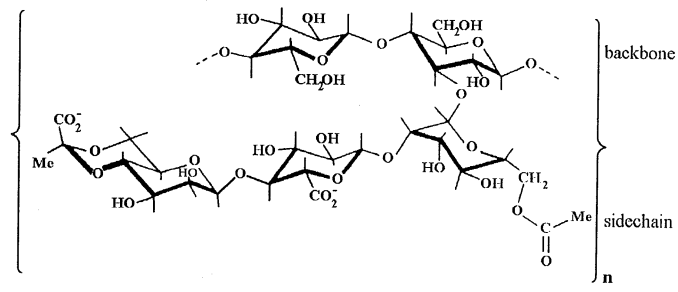

Figure 1. Primary structure of Xanthan gum.

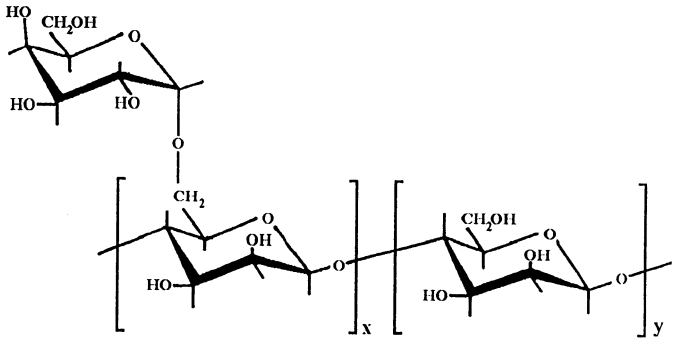

Figure 2. Basic structure of galactomannans. In locust bean gum, y = 3 or 4.

coils and in the condensed phase as stiff, extended ribbons, namely the galactomannans. Probably, the most well known example of this gelling, synergistic interaction is between xanthan and locust bean gum (LBG) (see Figure 2).

Indeed, concentrated aqueous systems of LBG and XG alone display quite different rheological properties: the former show the behaviour typical of hyperentangled macromolecular solutions, whereas the flow and viscoelastic properties of xanthan systems correspond to those of tenuous weak-gel networks. When mixed together, an interaction between the two polymer occurs which results in a firm, thermoreversible gel with synergistic effects, characterized by sharp setting and melting behaviour consistent with cooperative transitions and crosslinking by ordered non-covalent associations [4].

In more detail, the likely mechanism for the gelation between XG and LBG is generally believed to occur via the formation of mixed junction zones, the precise nature of which is still an object of strong debate [3–13].

This study is concerned with a thorough investigation of both polymer concentration and temperature effects on the rheological behaviour of mixed XG/LBG systems under continuous and oscillatory flow conditions, and the results are discussed with reference to the proposed models for the xanthan/galactomannan interaction.

Experimental

Materials

Commercial xanthan gum (Keltrol T, Kelco Inc.) and locust bean gum (Genu Gum type RL-200, Copenhagen Pectin Inc.) were separately dispersed, at 25 °C and under vigorous stirring, in a 20 mM KCl-bidistilled water solution with 0.005 $g l^{-1}$ of sodium azide added to each preparation to prevent bacterial degradation. The resultant solutions were autoclaved at 120 °C, centrifuged at 8000 rpm, filtered and allowed to rest overnight. The polymer concentration in each preparation was assessed by weight analysis on freeze-dried portions of the stock solutions. The solutions were then dialyzed against the same KCl solution, centrifuged again at 8000 rpm and filtered, and the final polymer concentration in each solution was determined again by weight analysis on freeze-dried portions.

The mixed systems (LX) were prepared, at different polymer ratios but constant total polymer concentration (1% by weight), by mixing a weighted amount of each batch polysaccharide system and appropriate dilution with the dialyzate solution.

Methods

All rheological measurements were performed with two rotational rheometers, the Haake RV100 and the Haake RV20, both coupled with the measuring device CV100, mounted with a coaxial cylinder sensor system ZB15 (Couette type).

The inner cylinder used with this coaxial sensor system has the following dimensions: 13.91 mm diameter, 32.30 mm length; the gap was 0.545 mm. During the tests, while the outer cup is driven, the inner cylinder is mechanically positioned and centred by an air bearing. The top and bottom surfaces of the inner cylinder are especially designed to minimize end effects.

Additional sets of experimental data were obtained, in oscillatory shear flow regime, with a sensitive prototype cone-and-plate rheometer for low deformation measurements, designed and constructed by Dr Robert K. Richardson of the Department of Food Research and Technology, Silsoe College, Bedford UK.

Stepwise procedures were applied for the analysis of the shear- and time-dependent properties in continuous shear flow conditions.

The multiple-step procedure consists of a sequence of different shear rates, each shear rate being kept constant until a steady value of the shear stress is attained. The analysis of the shear-dependent properties can then be properly based upon the steady values of the shear stress obtained at the different shear rates, whereas the sequence of stress transients allows an inspection of the nature and the extent of the time-dependent properties to be performed.

It is important to emphasize here that the relationship between the shear rate and the shear stress τ (that is, the shear viscosity η) can be obtained from the raw experimental data only in the case of Newtonian fluids. Indeed, for non-Newtonian systems it is necessary to consider the existence of a shear rate distribution in the gap and hence to calculate the 'effective shear rate' at the inner cylinder wall. Starting for the integral equation which relates the angular velocity Ω to the effective shear rate:

$$\Omega = \int_{\tau_0}^{\tau_i} \dot{\gamma}(\tau)/2\tau \, d\tau \tag{1}$$

a number of approximate methods have been proposed in literature for calculating shear rates in coaxial cylinder viscometers. In this paper, we used the method suggested by

Yang and Krieger [14], which is based on the derivation of both members of the above integral equation and on an expression of $\gamma(\tau)$ as a truncation of a convergent infinite series. In particular, the effective shear rates have been calculated according to the truncated form given by eqn (7) in the Yang and Krieger paper, and the corresponding values have been reported throughout this work.

Flow curves (shear stress vs effective shear rate plots) were fitted by using computerized non-linear regression analysis.

Dynamic measurements were carried out to investigate the viscoelastic properties of these materials. During the tests in oscillatory flow conditions, the shear strain γ imposed on the material is described by the following expression:

$$\gamma = \gamma^0 \sin(\omega t) \tag{2}$$

where t is the time, ω is the frequency of oscillation and γ^0 is the maximum shear strain. In the linear viscoelastic regime, a sinusoidal stress response of the same frequency, having amplitude τ^0 and phase lag δ, is obtained, so that the dynamic moduli G′ and G″ can be derived straight from the experimental data. When the applied strain exceeds a critical value, the viscoelastic behaviour becomes nonlinear, and the resultant periodic shear stress can be properly expressed by the Fourier series:

$$\tau = \gamma^0 \sum_{k,odd} [G'_k \sin(kt) + G''_k \cos(kt)] \tag{3}$$

in which each of the k harmonics is characterized by the coefficients G'_k and G''_k. With increasing strain, the weight of higher order harmonics, and specifically of the third harmonic, may become substantial; nevertheless, if the ratio of the amplitude of the third and fifth harmonic does not exceed 5%, the in-phase and the out-of-phase components of the fundamental harmonic, G'_1 and G''_1, can still be used to characterize, albeit with a certain degree of approximation, the elastic and viscous contribution to the entire response of the material [2].

Calibration of the apparatus was performed by carrying out measurements on Newtonian fluids, in order to evaluate both the response linearity of these systems under the selected operative conditions and to develop a standard procedure for the correction of the inertial effects. The strain dependence of the viscoelastic quantities for all systems was investigated with the prototype rheometer through strain sweeps in the range 0.0001–0.1 at a fixed frequency of oscillation of 10 rad s^{-1}, whereas an analysis of the transition from linear to nonlinear viscoelastic regime was performed by carrying out strain sweeps (from 0.05 to 2.5) at a constant frequency of 6.3 rad s^{-1} by using the Haake RV20-CV100 configuration. Frequency sweeps in the range 0.1–100 rad s^{-1} were performed at a constant strain value of 0.02.

Temperature sweeps in the range 25–85 °C were performed on all systems with the prototype rheometer at constant strain (0.02) and constant frequency of oscillation (1 rad s^{-1}), with a heating/cooling rate of 1 °C min^{-1}.

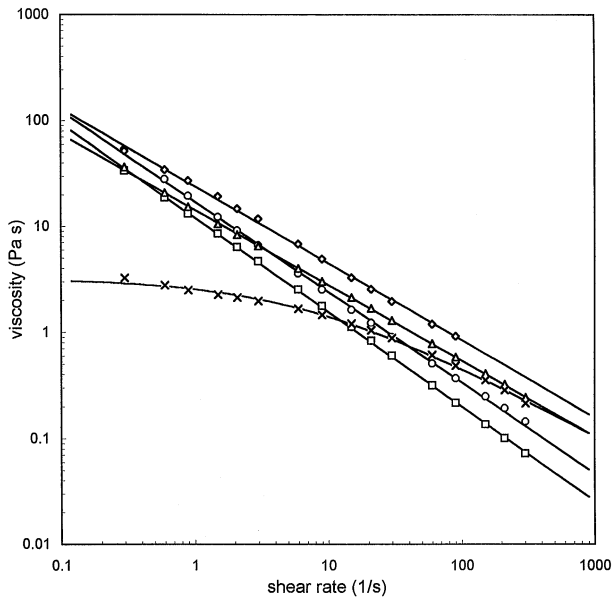

Figure 3. Steady shear flow behaviour of XG, LBG and all mixed systems (LX) at 25 °C: (×), LBG; (□), XG, (△), LX 1 : 3; (◇), LX 1 : 1; (○), LX 1 : 3. Continuous lines: data fitting with the Cross model (LBG) and the power-law model (other systems).

Results and discussion

Steady shear flow behaviour

The flow curves obtained from the application of the stepwise procedure at 25 °C to the XG, LBG and the mixed systems LX are reported in Figure 3. The flow properties of the pure LBG are those typical of a macromolecular solution, with a shear-thinning behaviour and a Newtonian region at low shear rates. Such behaviour, examplified in Figure 3, can be well approximated by the Cross model [15]:

$$\tau = \eta_\infty \dot{\gamma} + \frac{(\eta_0 - \eta_\infty)\dot{\gamma}}{1 + (\lambda\dot{\gamma})^m} \tag{4}$$

where η_0 is the zero-shear-rate viscosity (lower Newtonian pleateau), η_∞ is the infinite shear-rate viscosity (upper Newtonian plateau) λ is a characteristic time and m is a numerical exponent.

Conversely, the flow curves of pure xanthan and all relevant mixes are noticeably different. The rheological behaviour is still shear-thinning, but with no tendency towards a lower Newtonian plateau (see Figure 3), and can be suitably described by the power-law equation:

$$\tau = k\dot{\gamma}^n \tag{5}$$

where k is the consistency factor and n is the power-law exponent.

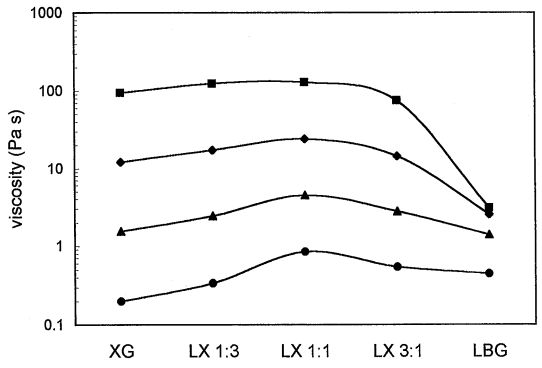

Figure 4. Mixing effect on steady shear viscosity: (■), $\dot{\gamma} = 0.1\ 1\ s^{-1}$; (◆), $\dot{\gamma} = 1\ 1\ s^{-1}$; (▲), $\dot{\gamma} = 10\ 1\ s^{-1}$; (●), $\dot{\gamma} = 100\ 1\ s^{-1}$.

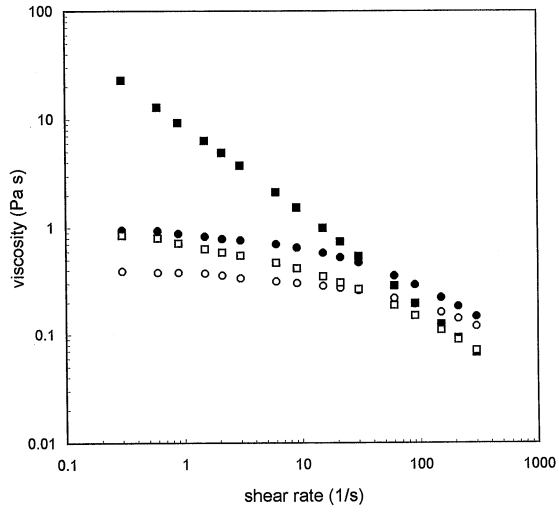

Figure 5. Steady shear viscosity of LBG and XG at 85 °C and 25 °C. $T = 25$ °C: (○), LBG; (□), XG. $T = 85$ °C: (●), LBG; (■), XG.

Moreover, the apparent viscosity at low shear rates is significantly higher than that for the LBG alone, even at the lowest XG : LBG ratio of (1 : 3). A closer inspection of data reveals also that the viscosity values do not increase monotonically with increasing xanthan concentration, but the synergistic effect has a maximum in correspondence of the XG : LBG ratio of 1 : 1. Figure 4 shows this mixing effect on the steady shear viscosity of these systems; it is evident from Figure 4 that the synergy becomes more and more pronounced as the shear rate decreases. The effect of temperature on the steady shear behaviour of xanthan and locust bean gum alone is reported in Figure 5. Whilst the flow curve for LBG at 25 and 85 °C do not show any qualitative change but there is only a parallel, downward shift of viscosity values with increasing temperature, as expected for a macromolecular solution, in the case of xanthan there is a dramatic change in the corresponding curve profiles. Indeed, at 25 °C and 20 mM KCl, the ordered chain sequences in the xanthan macromolecule are associated in extended junction zone, which span the entire sample in the three-dimensions and give rise to a weak-gel state, which is easily broken down under the action of shear, allowing the system to flow homogeneously, with marked non-Newtonian properties, strictly connected with the progressive disruption of the network into smaller flow units as the shear rate is increased. By increasing temperature, however, the xanthan molecule undergoes a thermally induced helix-coil conformational transition. The transition midpoint temperature, T_m, is a linear function of the ionic strength and, as reported in [5], the value of T_m corresponding to a 20 mM KCl solution should be comprised between 73 and 85 °C. Therefore, the flow behaviour of XG at 85 °C reported in Figure 5 corresponds to that of a system made up by xanthan molecules in the random coil confirmation and the flow curve shows the existence of a Newtonian plateau, followed by a shear-thinning zone. Such rheological behaviour is expected for single, flexible random coils that show far less anisotropy and shear orientation than the rigid helices.

Oscillatory flow behaviour at 25 °C

A preliminary step in the analysis of any oscillatory flow data should consist of checking the independence of instrumental responses of oscillation amplitude, i.e., the limit of the linear viscoelastic regime. As the strain increases, the system response remains unchanged in terms of amplitude, expressed through the complex modulus G*, and of the phase lag δ (= arctg G″/G′). At a certain point, a critical strain value is attained, above which we observe a progressive reduction of G*, whereas δ begins to increase. The critical strain then marks the limit of the viscoelastic regime within which it is possible to express, with a correct formalism, the entire material response in terms of G* and δ or, alternatively, of the elastic and viscous components of G*, the storage modulus G′ and the loss modulus G″, respectively.

Figure 6 reports the results obtained from a strain sweep performed at constant frequency of oscillation of 6.3 rad s^{-1} in a deformation range from 0.05 to 2.5 on the LBG, XG and all LX mixed systems. Figure 6 clearly shows the effects of xanthan addition on the extension of the linear viscoelastic regime, and on the strain dependence in the nonlinear region.

The critical strains for the LBG and XG systems are typical of polymer solutions and weak gels, respectively [2].

Interestingly, the mixed systems show higher sensitivity to strain amplitude, and lower strain values must be attained to ensure linear viscoelastic properties. In fact, adding even small amounts of xanthan to the initial locust bean gum solution causes a sharp increase in the values of the complex modulus G*, along with a variation in the shape of the G* curve. Once again, the maximum effect of the interaction between XG and LBG is observed for the system with XG : LBG ratio of 1 : 1 which, consequently, represents a critical condition for mixing. The extreme

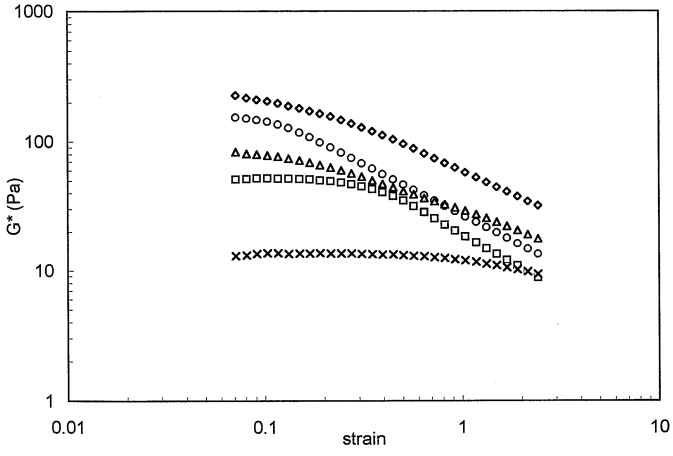

Figure 6. Complex modulus G* vs strain at $\omega = 6.28\,\text{rad}\,\text{s}^{-1}$ and $T = 25\,^{\circ}\text{C}$: (×), LBG; (□), XG; (△), LX 3 : 1; (◇), LX 1 : 1; (○), LX 1 : 3.

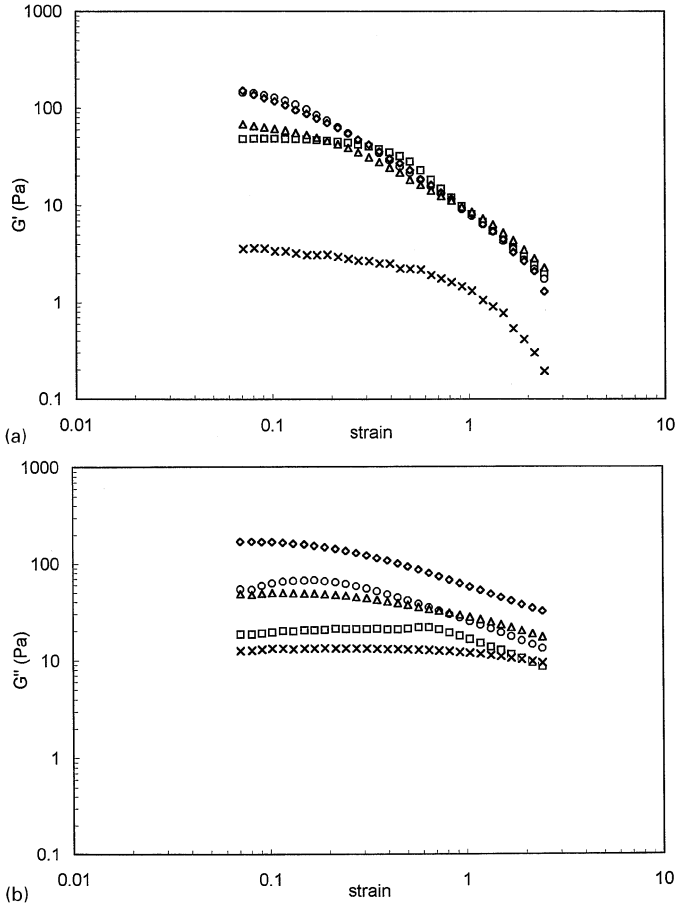

Figure 7. Storage modulus (a) and loss modulus (b) vs strain at $\omega = 6.28\,\text{rad}\,\text{s}^{-1}$ and $T = 25\,^{\circ}\text{C}$: (×), LBG; (□), XG; (△), LX 3 : 1; (◇), LX 1 : 1; (○), LX 1 : 3.

sensitivity to imposed strain could be reasonably ascribed to the existence of the mixed junction zones in the gel systems, whose heterogeneous nature allows them to be easily broken down by the action of stress.

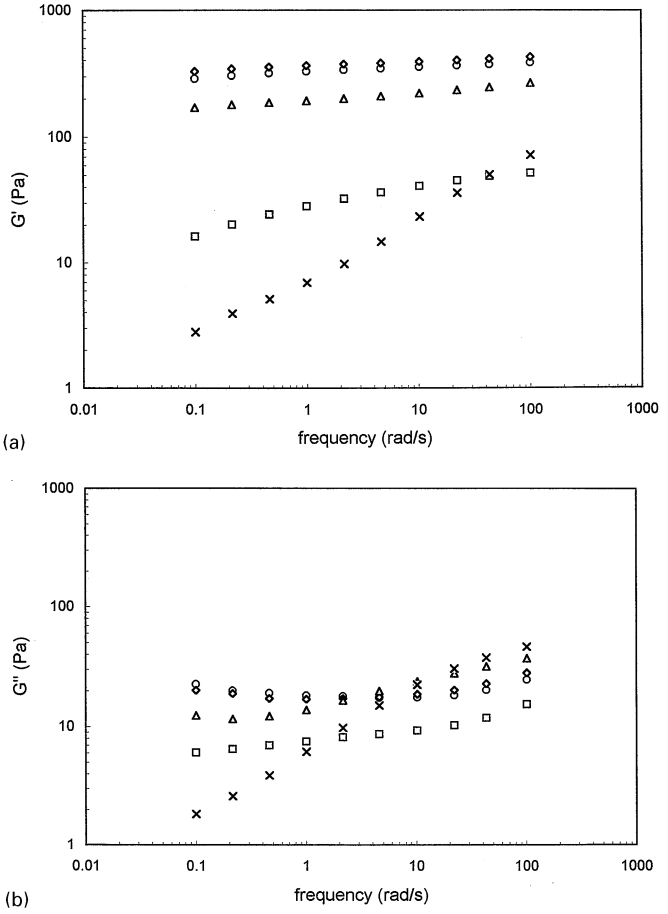

Figure 8. Storage modulus (a) and loss modulus (b) vs frequency at $\gamma = 2\%$ and $T = 25\,^{\circ}\text{C}$: (×), LBG; (□), XG; (△), LX 3 : 1; (◇), LX 1 : 1; (○), LX 1 : 3.

When both elastic and viscous components are examined, a typical transition from linear to nonlinear behavior is generally observed for all systems: as a general rule for both solutions and weak gels, G′ departs from linearity sooner and more rapidly than G″ (see Figures 7a and b).

As concerns the dependence of the viscoelastic quantities G′ and G″ on the imposed frequency of oscillation, Figures 8a and b show the corresponding profiles of G′ and G″ for the XG, LBG and all LX mixed systems considered. These mechanical spectra clearly show the influence of composition on the viscoelastic properties of these biopolymer systems. The XG spectrum (Figure 9a) illustrates that, when subjected to the small deformation applied during the measurements (2% strain), this biopolymer behaves as a weak gel: the storage modulus G′ is greater than the loss modulus G″ in the entire frequency window explored, and both viscoelastic quantities show only a slight dependence on the imposed frequency of oscillation. At the other extreme, the LBG spectrum (Figure 9b) is closer to that exhibited by concentrated polymer solutions, with both G′ and G″ strongly dependent upon the imposed frequency,

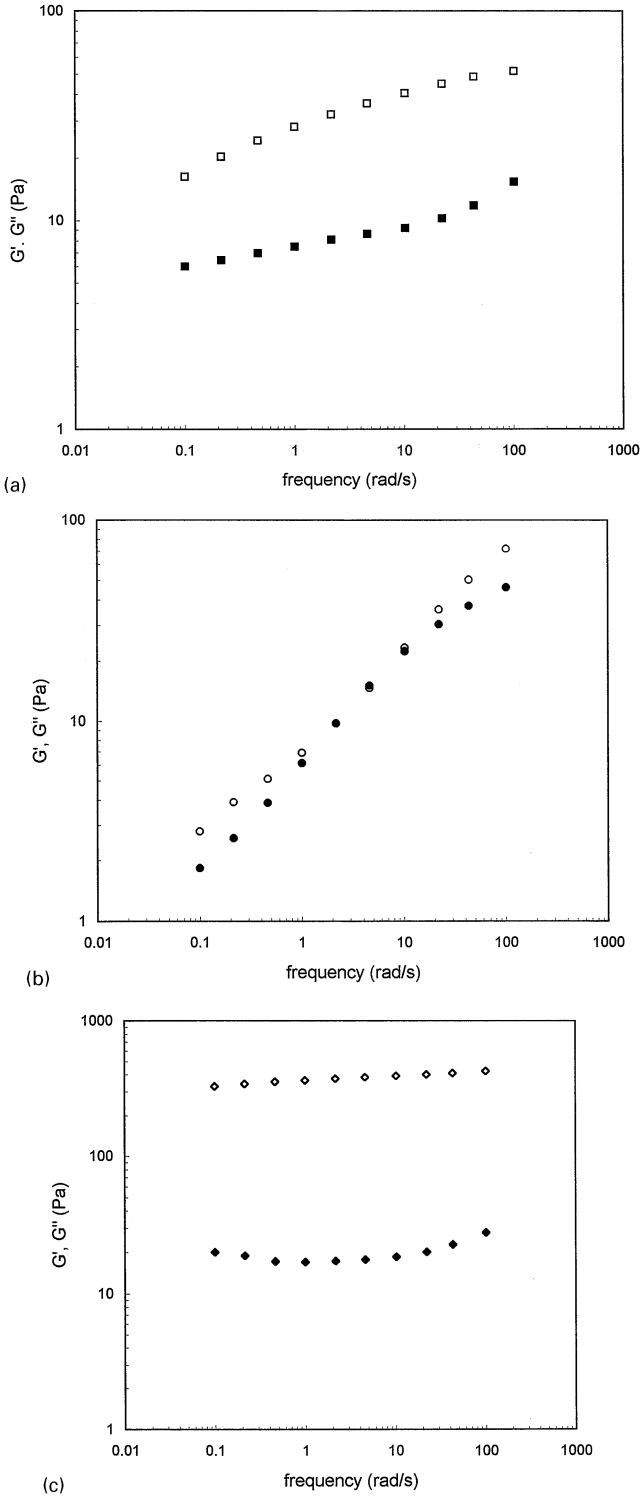

Figure 9. Mechanical spectra at $\gamma = 2\%$ and $T = 25\,^{\circ}C$. (a): XG, (□), G′, (■), G″; (b): LBG, (○), G′, (●), G″; (c): LX 1 : 1, (◇), G′, (◆), G″.

even if the low frequency behaviour of this system seems to suggest that the polymer has not reached the state of a 'true' molecular solution. All mixed systems show the mechanical spectra typical of polysaccharide gels: G′ is always much

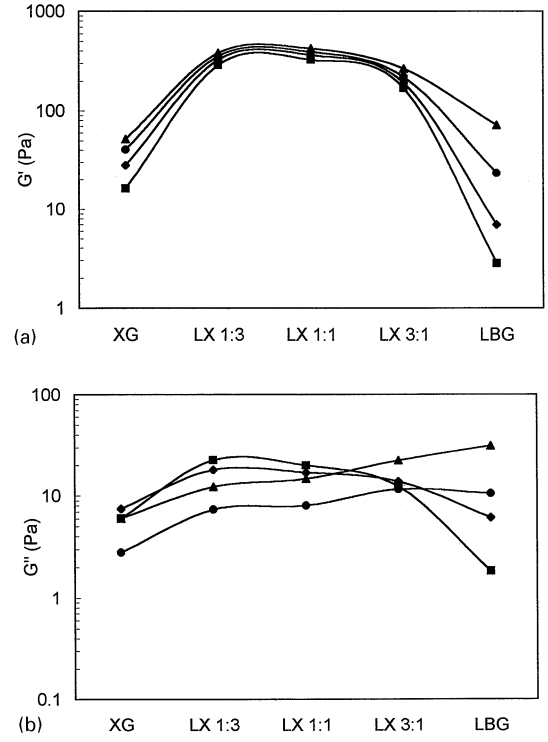

Figure 10. Mixing effect on storage modulus (a) and loss modulus (b) at $\gamma = 2\%$ and $T = 25\,^{\circ}C$. (■), $\omega = 0.1\ rad\,s^{-1}$, (◆), $\omega = 1\ rad\,s^{-1}$; (●), $\omega = 10\ rad\,s^{-1}$, (▲), $\omega = 100\ rad\,s^{-1}$.

greater than G″ and is nearly independent of the applied frequency over a wide frequency range. Moreover, as for other biopolymer gels [2], the profile of G″ shows a slight minimum in the experimental frequency window explored. Once again, Figures 8a and b indicate how the mixed system LX 1 : 1 mechanical spectrum (see Figure 9c for detail) can be considered as resulting from the strongest synergistic behaviour. In addition, the marked gap between the elastic responses of the pure LBG and the LX 1 : 3 systems demonstrates the strong effect of the initial addition of xanthan to the pure LBG, especially in the low frequency range. This can be considered as an evidence for the transition from sol to gel behaviour.

The synergistic interaction between XG and LBG is better illustrated by Figures 10a and b, which show how the dynamic rheological quantities vary with the applied frequency for all the systems considered. Figure 10a clearly demonstrates that the interaction occurring when XG and LBG are mixed at 25 °C results in significantly enhanced values of the relevant storage modulus. The loss modulus alters little (see Figure 10b), suggesting that the synergistic effect can be tentatively interpreted as an increase in the density of crosslinks between the two polysaccharides. Moreover, as the applied frequency decreases, the extent of the synergistic effect increases by virtue of the formation of long-range structures within the mixed systems.

Table 1. Values of the parameters of the Friedrich model.

System	G_e *(Pa)*	G_m *(Pa)*	a
LBG	1.64	192.8	0.59
LX 3 : 1	155.9	241.5	0.32
LX 1 : 1	198.22	461.2	0.11
LX 1 : 3	0	779.5	0.06
XG	0	122.2	0.23

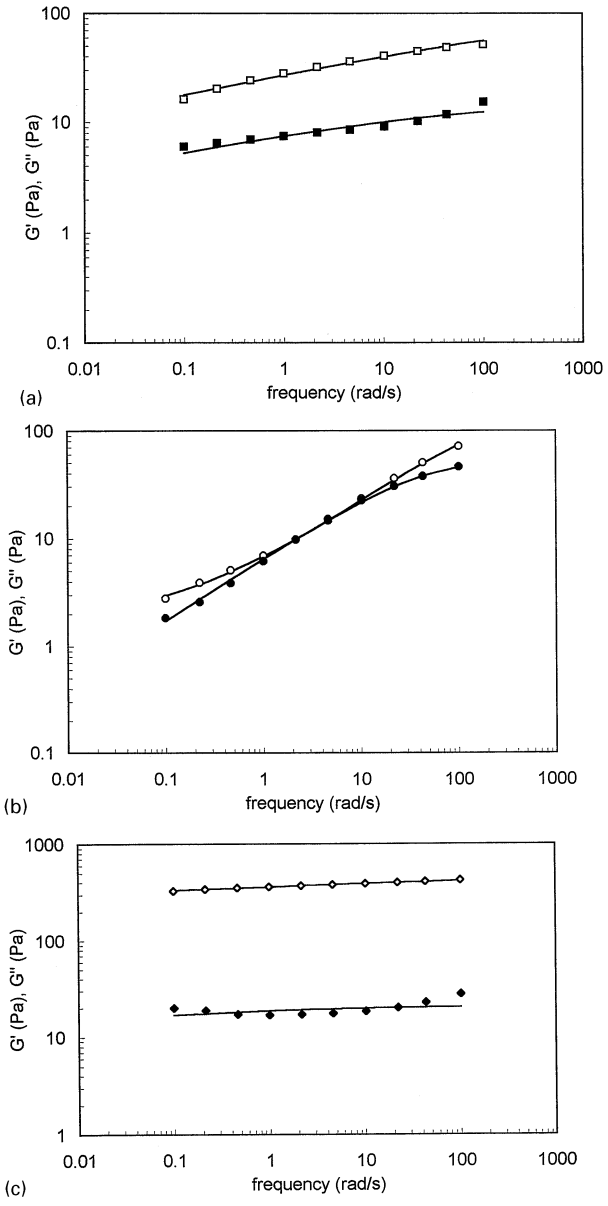

Figure 11. Fitting of the mechanical spectra reported in Figures 9a, b and c with the Friedrich model. (a), XG; (b), LBG; (c), LX 1 : 1.

A comprehensive description of the frequency dependence of both moduli can be suitably obtained through the four-parameter Friedrich model, which belongs to the class of the fractional derivative approaches to viscoelasticity [16]:

$$G'(\omega) = G_e + G_m \frac{y^a\left[\cos\left(a\frac{\pi}{2}\right) + y^a\right]}{1 + 2y^a\cos\left(a\frac{\pi}{2}\right) + y^{2a}} \qquad (6')$$

$$G''(\omega) = G_m \frac{y^a\sin\left(a\frac{\pi}{2}\right)}{1 + 2y^a\cos\left(a\frac{\pi}{2}\right) + y^{2a}} \qquad (6'')$$

where G_e is the equilibrium modulus, G_m represents the difference between the two limiting values of G′ (*ie* at very low and very high oscillation frequency, respectively), a is the order of the fractional derivative, ranging between 0 (viscoelastic solid behaviour) and 1 (viscoelastic liquid behaviour), and $y = \lambda \times \omega$, in which λ is the relaxation time and ω is the oscillation frequency. Data fitting was performed keeping the relaxation time λ constant and equal to 0.005 s, in order to overcome the problem of the strong correlation between the parameters λ and a. Table 1 shows the values of the Friedrich parameters for the XG, LBG and all LX mixed systems examined. The low value of a, along with the high G_e value underline the solidlike characteristics of the LX 1 : 1 system.

Figures 11a, b and c report, as an example, the results of the fitting of the experimental data with the Friedrich model for the XG, LBG and LX 1 : 1 systems, respectively.

Thermal effects

As the temperature is increased from 25 °C to 85 °C, the same thermal effect is observed for the XG and all LX mixed systems considered, indicating a progressive change from the behaviour of a typical gel to that of a quasi-solution state. Figures 12a and b illustrate the mechanical spectra of the two extreme systems LBG and XG respectively, at 85 °C. Whereas the LBG spectrum shows only a quantitative change in the values of the moduli with respect to the spectrum recorded at 25 °C, as expected for polymer solutions, the spectrum of XG is entirely different from that exhibited by the same polymer at 25 °C: indeed, 85 °C is well above the transition midpoint temperature for XG, so that the corresponding mechanical spectrum of XG is now that of a random coil polymer solution.

The gel-sol transition for the mixed systems is well exemplified by the mechanical spectra reported in Figures 13a and b for the LX 1 : 1 system, whereas Figure 14a brings together the effects of temperature and applied frequency of oscillation on the total stress response G* of this system. The contribution of the viscous component to G* becomes more and more pronounced as the temperature increases, as can be seen from Figure 14b, which reports the behaviour of the loss tangent (G″/G′) as a function of temperature and frequency.

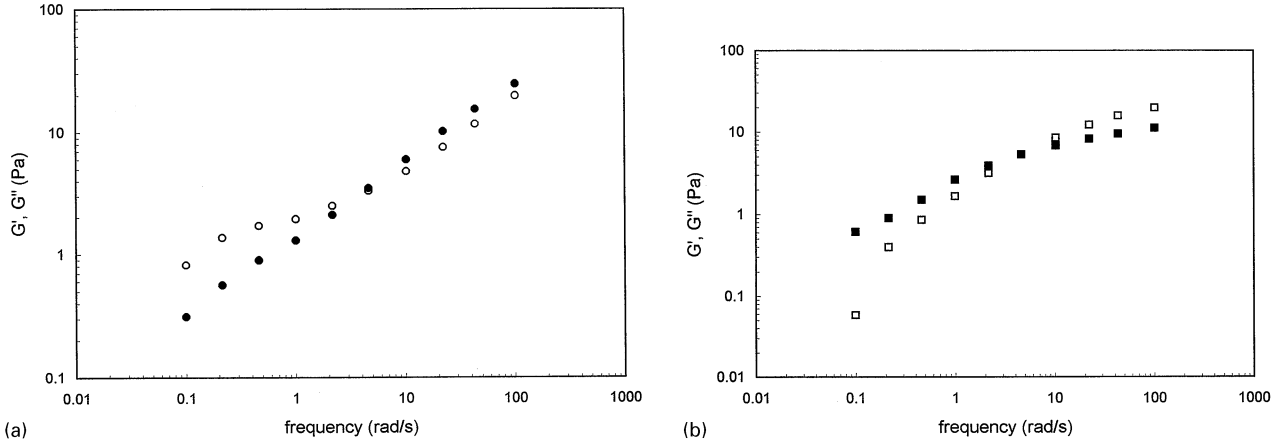

Figure 12. Mechanical spectra of LBG and XG at $\gamma = 2\%$ and $T = 85\,^{\circ}C$. (a): LBG, (○), G′, (●), G″; (b): XG, (□), G′, (■), G″.

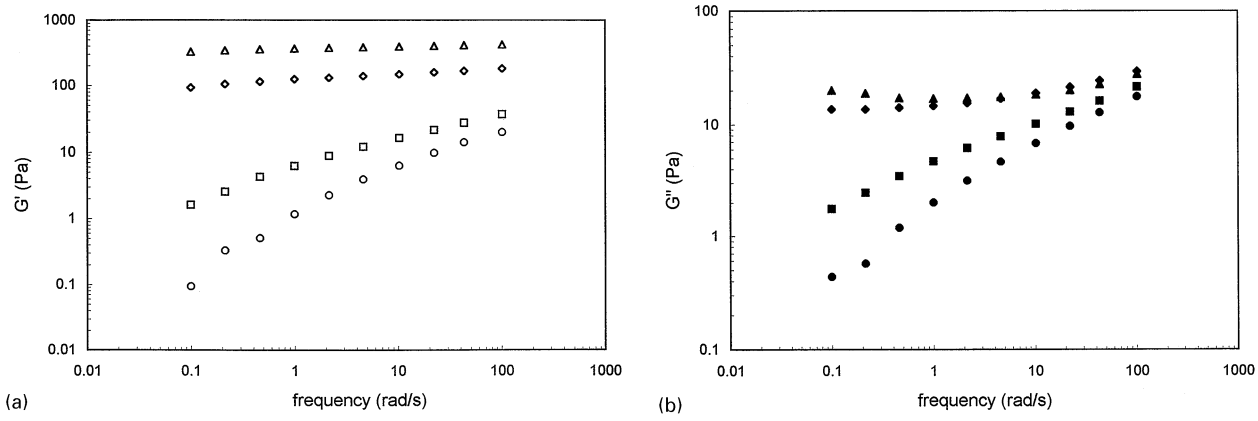

Figure 13. Effect of temperature on the storage modulus (a) and loss modulus (b) for the LX 1 : 1 system at $\gamma = 2\%$. (a), G′, (○) , $T = 85\,^{\circ}C$; (□), $T = 65\,^{\circ}C$; (◇), $T = 45\,^{\circ}C$; (△), $T = 25\,^{\circ}C$. (b), G″, (●), $T = 85\,^{\circ}C$; (■), $T = 65\,^{\circ}C$; (◆), $T = 45\,^{\circ}C$; (▲), $T = 25\,^{\circ}C$.

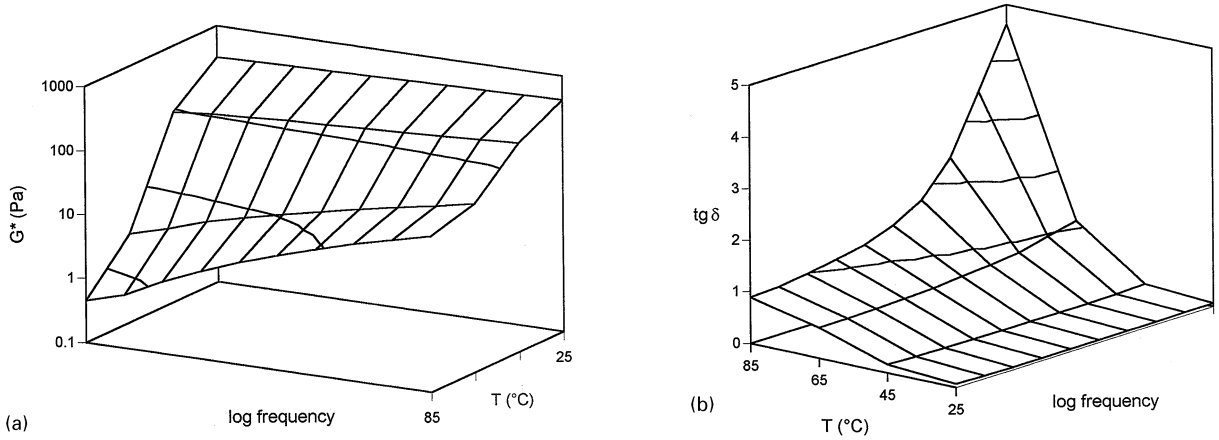

Figure 14. Combined effects of temperature and frequency of oscillation on the complex modulus G* (a) and the loss tangent δ (b) for the LX 1 : 1 system. $\gamma = 2\%$.

Among all mixed systems, the LX 1 : 1 has the highest values of the moduli at any temperature considered, and is characterized by the highest gel-sol transition temperature. This can be easily inferred from the data reported in Figures 15a and b, which show the behaviour of G* and δ as a function of increasing temperature T for the LBG, XG and all LX mixed systems considered. It must be noted here that the curves obtained on cooling the samples through the

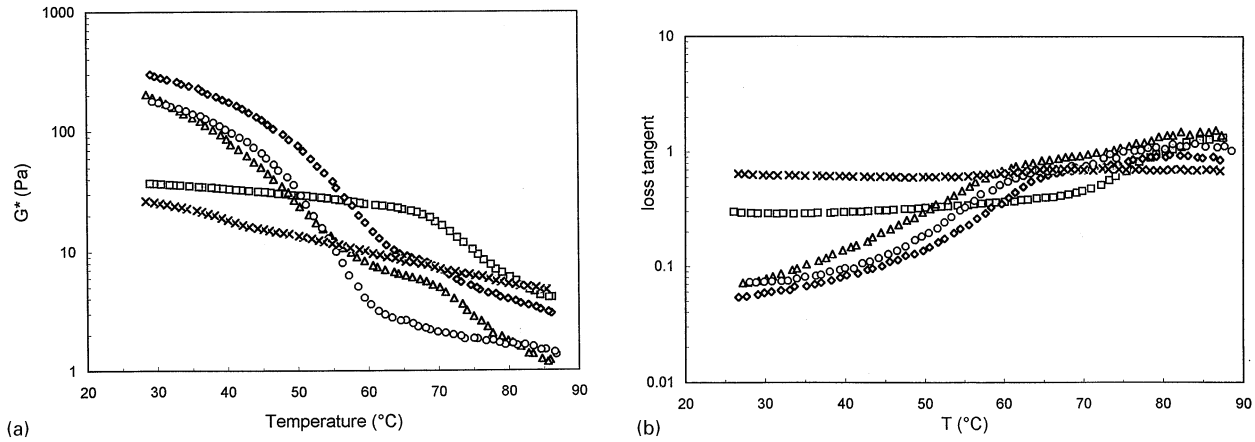

Figure 15. Effect of temperature on the complex modulus G* (a) and the loss tangent δ (b) at constant $\omega = 1$ rad/s and $\gamma = 2\%$. Cooling rate: 1 °C/min. LBG (×); XG (□); LX 1:3, (○); LX 1:1, (◇); LX 1:3, (△).

sol-gel transition were virtually identical (*ie* with no discernible thermal hysteresis between melting and gelation). A detailed inspection of Figure 15a reveals that, for the LBG solution, the values of G* slowly and regularly decrease with increasing T from 25 °C to 85 °C, whereas the curve of G* *vs* T for XG has a sigmoidal shape, with the inflection point corresponding to ~75 °C. This temperature value falls nicely in the interval 73–85 °C, within which the helix-coil transition midpoint temperature T_m for xanthan in 20 mM KCl should be comprised. As expected, this conformational transition results in a sensible reduction of the elastic features of this system, as well evidenced in Figure 15b.

Noticeably, the temperature sweeps performed on the three LX mixed systems clearly show that, in these cases, the gel-sol transition follows a two-step process, characterized by the presence of two inflection points in the relevant G* *vs* T curves. The first step could be reasonably ascribed to the melting process of the mixed xanthan-locust bean gum junction zones, in which the association of XG with LBG is occurring with the xanthan component in its fully ordered helical conformation. The temperatures of the first inflection points are ~53 °C for the LX 1:3, ~56 °C for the LX 3:1 and ~58 °C for the LX 1:1, respectively. Besides further evidence for maximum synergy in LX 1:1, the decrease in synergistic interaction (*ie* the lower melting temperature) for the mixed system with the highest xanthan context (LX 1:3) can be explained, according to what proposed by Morris [10], by considering that, since the xanthan is already stuck to itself, it has less capacity to stick to anything else and, the more xanthan is locked in an aggregate state, the less it will be able to adjust its conformation to the geometry required for efficient packing within heterotypic junction zones.

The second step, occurring at higher temperature, can be attributed to the conformational transition of the xanthan chains.

Conclusions

The results of this study evidence that, when the microbial polysaccharide xanthan gum and the plant galactomannan locust bean gum are mixed at room temperature and under 20 mM KCl conditions, the two biopolymers interact to form synergistic mixed gels, whose mechanical spectra resemble those of strong gels but the continuous shear flow properties are not far from those exhibited by the weak-gel xanthan system alone.

These observations, coupled with the results obtained from temperature sweeps, seem to suggest the coexistence, within the structure of these mixed gels, of both heterotypic LBG-XG and homotypic XG-XG junction zones, in which the xanthan chains retain their ordered helical conformation, thus supporting the original model described by Dea *et al.* [4] and Morris *et al.* [11].

Acknowledgements

We thank Professor E.R. Morris and Dr R.K. Richardson for the helpful discussions and the generous access to the prototype rheometer. We also thank Dr G. Sanderson of the Kelco Division of Merck & Co., Inc. and Dr Claus Rolin, of the Copenhagen Pectin, Inc. for the polysaccharide sample gifts.

References

1 McKay JE, Stainsby G, Wilson EL (1985) *Carbohydr Polym* **5**: 223–35.
2 Lapasin R, Pricl S (1995) *Rheology of Industrial Polysaccharides*: *Theory and Applications* Blackie/Chapman & Hall: Glasgow.
3 Morris ER (1990) In *Food Gels*, Harris P (ed) pp 291–359. London & New York: Elsevier Science Publishers.
4 Dea ICM, Morris ER, Rees DA, Welsh EJ, Barnes HA, Price J (1977) *Carbohydr Res* **57**: 249–72.

5 Norton IT, Goodall DM, Frangou SA, Morris ER, Rees DA (1984) *J Mol Biol* **175**: 371–94.
6 Dea ICM, Clark AH, McCleary BV (1986) (a) *Carbohydr. Res.* **147**: 275–94. (b) *Food Hydrocoll.* **1**: 129–40.
7 Tako M, Asato A, Nakamura S (1984) *Agric Biol Chem* **48**: 2995–3000.
8 Cairns P, Miles MJ, Morris VJ, Brownsey GJ (1987) *Carbohydr Res* **160**: 411–23.
9 Cheetham NWH, Mashimba ENH (1988) *Carbohydr Polym* **9**: 195–206.
10 Morris ER, Foster TJ (1994) *Carbohydr Polym* **23**: 133–5.
11 Morris ER, Rees DA, Young G, Walkinshaw MD, Darke A (1977) *J Mol Biol* **110**: 1–16.
12 Zhan DF, Ridout MJ, Brownsey GJ, Morris VJ (1993) *Carbohydr Polym* **21**: 53–8.
13 Mannion RO, Melia CD, Launay B, Cuvelier G, Hill SE, Harding SE, Mitchell JR (1992) *Carbohydr Polym* **19**: 91–7.
14 Yang TMT, Krieger IM (1978) *J Rheol* **23**: 413–21.
15 Cross MM (1965) *J Colloid Sci* **20**: 417–24.
16 Friedrich Chr (1991) *Rheol Acta* **30**: 151–8.

Received 19 March 1996, accepted 4 June 1996